ADSORPTION IN ELECTRONIC NOSE

URBAN PEČOLER

Fakulteta za matematiko in fiziko Univerza v Ljubljani

Adsorption is a process in which molecules adhere to the surface of a solid phase. Various theoretical models describe this phenomenon depending on the surface properties and the chemical identity of the adsorbate. Adsorption plays a significant role in numerous fields, including electronic sensing. This article presents the Langmuir adsorption model, its modifications, and a comparison with experimental data. Furthermore, the role of adsorption in capacitive gas sensors is examined, focusing on a electronic nose device developed at Jožef Stefan Institute. Finally, potential improvements using porous materials such as metal-organic frameworks are discussed, highlighting their potential for enhancing sensitivity and selectivity in future sensor designs.

ADSORPCIJA V ELEKTRONSKEM NOSU

Adsorpcija je proces, pri katerem se molekule vežejo na površino trdne faze. Različni teoretični modeli opisujejo ta pojav glede na lastnosti površine in kemijsko identiteto adsorbenta. Adsorpcija ima pomembno vlogo na številnih področjih, med drugim tudi pri elektronskem zaznavanju. V tem članku je predstavljen Langmuirjev adsorpcijski model, njegove modifikacije in primerjava modela z eksperimentalnimi podatki. Poleg tega je obravnavana vloga adsorpcije v kapacitivnih senzorjih plinov v elektronskem nosu, razvitem na Institutu Jožef Stefan. Na koncu so obravnavane možne izboljšave z uporabo poroznih materialov, kot so kovinsko-organska ogrodja, pri čemer je poudarjen njihov potencial za povečanje občutljivosti in selektivnosti v prihodnjih zasnovah senzorjev.

1. Introduction

Many physical and chemical processes take place at the boundary between a solid phase and a liquid or gas phase. These interfaces serve as active sites where numerous interesting phenomena occur, including molecular interactions, surface reactions, and adsorption. The process of adsorption is the adhesion of a chemical species onto the surface of a solid phase. It plays a vital role in various scientific disciplines and industrial applications, such as industrial separation processes [1] and food processing [2]. Recent research has focused on advancing our understanding of adsorbate-surface interactions and exploring new materials with tailored properties for specific applications. This includes porous materials such as metal-organic frameworks (MOFs) and zeolites [3], as well as carbon-based materials [4]. Additionally, high-resolution imaging techniques such as atomic force microscopy (AFM) [5] and scanning tunneling microscopy (STM) [6] have provided insights into the molecular-scale behavior of adsorbates on surfaces. A fundamental concept in adsorption science is the adsorption isotherm. It describes the relation between the quantity of adsorbed sample and the concentration or pressure in the bulk phase at some constant temperature. One of the aims of this article is to derive this isotherm for gas-solid systems and explore the modifications that can be made to that model. A notable area where adsorption plays a key role is in gas sensing. Various types of gas sensors rely on the adsorption of molecules onto a sensing layer, which induces a measurable physical or chemical change. For instance, metal oxide semiconductor (MOX) sensors involve both adsorption and chemical reactions, which modify the electrical resistance of the sensor [7]. Capacitive sensors, on the other hand, primarily rely on physical adsorption, resulting in a change in the dielectric environment that alters the sensor's capacitance. Among their various applications, these types of sensors are also used in electronic nose systems. The term electronic nose refers to a system designed to mimic the human sense of smell. It typically consists of an array

© © 2025 The Author(s). Original content from this work may be used under the terms of the Creative Commons Attribution 4.0 licence.

of partially selective gas sensors, whose combined output is processed using pattern recognition algorithms. A single gas sensor often lacks the selectivity needed to distinguish between similar compounds. However, by analyzing the combined response of multiple sensors to a gas mixture, an electronic nose can detect complex odor patterns with much greater specificity [8, 9]. This article focuses specifically on adsorption processes occurring in capacitive sensors used in electronic nose devices. Although traditionally electronic noses have relied heavily on MOX sensors, the use of nanoporous dielectric materials in capacitive sensors presents new opportunities in this field.

2. Fundamentals of adsorption

Many physical and chemical processes involve interactions at solid surfaces, where adsorption plays a critical role. Whether in catalysis, gas storage, or sensing applications, the ability of a surface to attract and retain molecules influences material behavior and functionality.

2.1 Definition and classification

Adsorption refers to the process where molecules from the gas phase or liquid solution adhere to the surface of a solid bulk phase. The reversal process is called desorption, where adhered molecules are removed from the surface. The molecules that bind to this surface are called adsorbates, while the material to which they bind is called as adsorbent. It is also important to note that in this regard the surface refers to the interfacial layer, which is a space region between two contacting bulk phases. In addition, the physical and chemical properties of the two phases at the interfacial layer must be significantly different, in density, polarity, or molecular interactions. A good example of this are solid-gas or solid-liquid systems.

Adsorption can be further divided into physisorption and chemisorption. The main difference between the two lies in the bonding energy with which molecules adhere to the surface. It is conventionally accepted that the energetic threshold separating these two types of adsorption is around 0.5 eV per adsorbed molecule [10]. Due to their larger binding energies, chemisorbed molecules form ionic, hydrogen, or covalent bonds, depending on the chemical identity of the adsorbate. These strong interactions can alter the molecular structure, and the molecule may lose its original chemical identity upon desorption. On the other hand, physisorption is characterized by much weaker interactions. The forces involved are primarily van der Waals interactions and electrostatic attractions, which are comparable in strength to other weak intermolecular forces. As a result, physisorbed molecules retain their chemical identity and are more easily reversible. Gas adsorption is typically classified as physisorption due to the nature of these weak interactions. We also have to distinguish between mono- and multi-layer adsorption. In the latter, multiple layers of adsorbate can form on the surface, whereas in monolayer adsorption, all adsorbate molecules are confined to a single layer in direct contact with the interfacial layer.

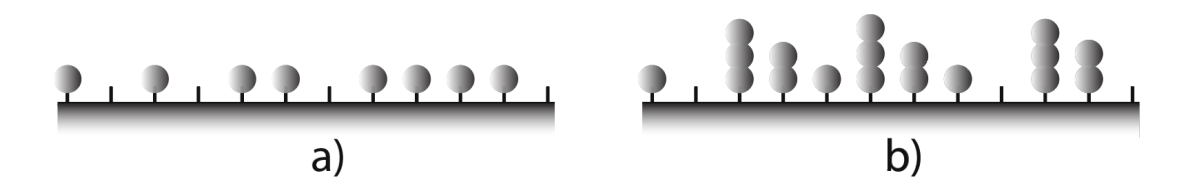


Figure 1. Illustration of adsorption mechanisms: a) monolayer adsorption (single-layer coverage of adsorbate molecules) and b) multilayer adsorption (successive layers of adsorbate forming on the surface).

Figure 1 illustrates mono-layer and multi-layer adsorption on adsorption sites of a flat surface. In multi-layer adsorption, molecules accumulate on top of one another due to strong intermolecular interactions between adsorbate molecules. These interactions are strong enough to overcome thermal agitation, which is characterized by the thermal energy scale $k_{\rm B}T$. This typically occurs when the system temperature is smaller or near the boiling point of the adsorbate at the given pressure. Monolayer adsorption, on the other hand, is usually dominated by interactions between the adsorbent and the adsorbate [11]. Physisorption on large open surfaces consists of a layer by layer filling process. The first layer is therefore filled when

 $\Theta = \frac{N_{\rm a}}{N_{\rm m}} = 1,\tag{1}$

where Θ is defined as the surface coverage, which tells us how many adsorption sites are already filled, $N_{\rm a}$ is the number of molecules adsorbed onto the surface and $N_{\rm m}$ represents the total number of adsorption sites. Adsorption sites are specific locations on a surface where molecules can bind or adhere due to attractive forces. There are several factors which determine the presence and characteristics of adsorption sites, like surface structure, chemical composition, and surface energy. We can define adsorption sites with molecules that adsorb on the surface. Therefore, one molecule can only occupy one adsorption site. We are dealing with mono-layer adsorption if $\Theta \leq 1$ and multi-layer adsorption if $\Theta > 1$. The adsorption behavior also strongly depends on the physical properties of the adsorbing molecules. Larger molecules generally have a greater surface area available for interaction, increasing their likelihood of adsorption. Additionally, molecules with higher area-to-volume ratios are more likely to adsorb. In the case of physisorption, where intermolecular forces govern the process, molecular polarity plays a crucial role. Polar molecules experience stronger electrostatic interactions with the surface, which can enhance both the rate and strength of adhesion.

2.2 Adsorption isotherm

Adsorption isotherms are commonly used to describe how the amount of adsorbate adhered to a surface depends on its concentration or pressure in the surrounding phase at a constant temperature. These mathematical models provide insight into how surface coverage varies with these conditions and are essential tools for interpreting adsorption measurements. For a given gas-solid system at fixed temperature T, the surface coverage Θ or in other words the amount of adsorbed gas per unit mass of adsorbent, is expressed as a function of the equilibrium pressure p:

$$\Theta = f(p)$$
.

The specific form of the function f(p) depends on the chosen adsorption model and the nature of the interaction between the gas molecules and the surface. Common models include the Langmuir isotherm for monolayer adsorption, and more complex models like the BET isotherm for multilayer adsorption [11]. Adsorption isotherms are greatly dependent on the geometry of a surface. The simplest adsorption models make an assumption that the surface is uniform and flat. However, in practice, we want to use materials with a high active surface area, which is the area available for adsorption of molecules. In other words, we want to use materials with a high number of adsorption sites $N_{\rm m}$. These materials are called porous materials, meaning solids with cavities or channels. We classify pores in a material into micropores, which are less than two nanometers wide, mesopores that are between two and 50 nanometers wide, and macropores that are more than 50 nanometers wide [12]. An example of a porous solid is metal organic frameworks, which we will explore more in chapter 3. Adsorption isotherms are generally classified into six types according to the International Union of Pure and Applied Chemistry (IUPAC) classification [13], each describing distinct adsorption behaviors based on the interactions between the adsorbate and adsorbent. Among these, Type I is the most relevant to this study, as it corresponds to the Langmuir adsorption model. This type is

characteristic of monolayer adsorption on microporous or non-porous materials, where adsorption increases rapidly at low pressures and subsequently plateaus as the available surface sites become saturated. Other isotherm types describe different adsorption mechanisms. Type II and Type III represent multilayer adsorption and weak adsorbate-adsorbent interactions, respectively, while Type IV and Type V are associated with mesoporous materials. Type VI, in contrast, describes stepwise multilayer adsorption on uniform surfaces.

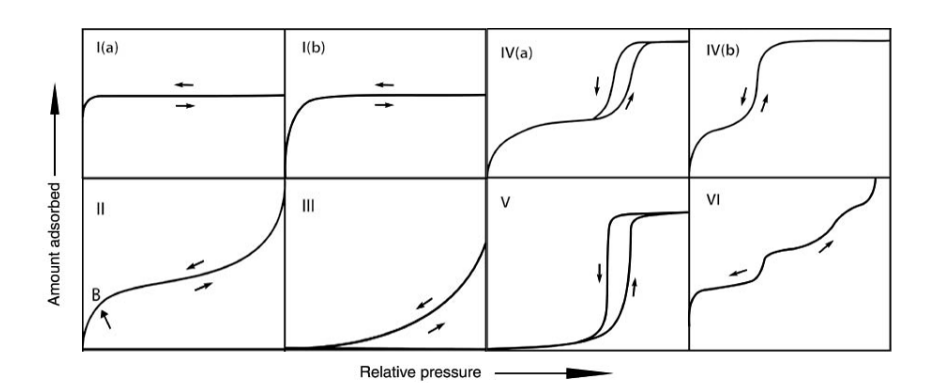


Figure 2. The six types of adsorption isotherms according to the IUPAC classification. The most relevant for this article is Type I, which follows the Langmuir adsorption model and is characteristic of microporous materials. The amount of adsorbed molecules (y-axis) depends not only on pressure but also on the density and availability of adsorption sites on the surface. Figure adapted from [13] with modified layout (reoriented by placing the lower half to the right). © IUPAC, De Gruyter (2015)

The classification of adsorption isotherms is shown in figure 2. This approach provides a fundamental framework for understanding adsorption behavior across different materials. Among these, Type I adsorption is particularly important due to its well-defined saturation behavior and its relevance in both theoretical and applied adsorption studies. Its predictability and simplicity make it a valuable model for describing adsorption processes in controlled environments, where monolayer coverage is the dominant mechanism.

3. Adsorption models

In the context of this article, we are primarily interested in systems where physical adsorption dominates, as is the case in capacitive sensors used in electronic nose devices. In such systems, adsorbed molecules can be removed from the sensor surface by purging with a flow of clean gas, which is useful for device baseline calibration without the need for heating or chemical cleaning. To get a simple idea of physisorption, we consider the example of nitrogen adsorption on graphite. Graphite consists of layers of carbon atoms arranged in a hexagonal lattice, forming a flat and relatively uniform surface. While not as high in surface area as porous materials, the structure offers many evenly distributed adsorption sites, making it a useful model system for studying adsorption phenomena. As nitrogen molecules approach the graphite surface, they interact with the carbon atoms via weak van der Waals forces, leading to the formation of an adsorbed monolayer. Although nitrogen is a nonpolar molecule, electron charge fluctuations within nitrogen atoms create a short-lived dipole moment, which in turn induces a dipole moment in the carbon atoms of graphite [14]. The density of nitrogen molecules on the graphite substrate is approximately one nitrogen molecule on every third graphite hexagon, as shown in figure 3.

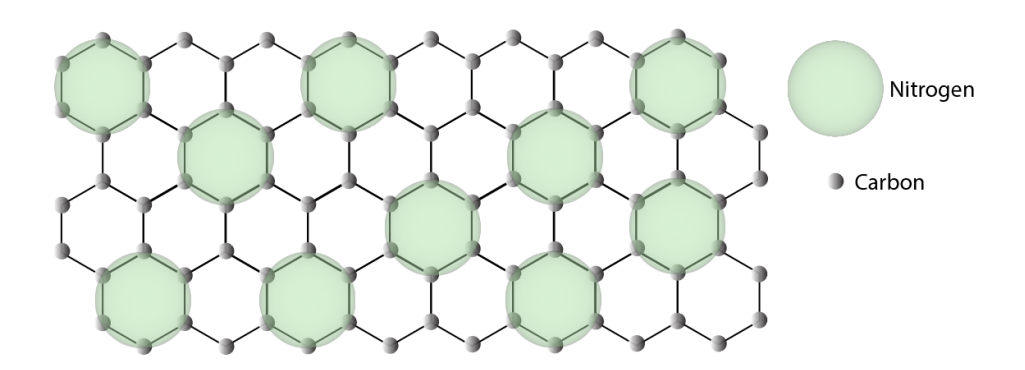


Figure 3. Schematic showing nitrogen molecules (green) adsorbing on graphene (carbon in gray) with a ratio of one nitrogen molecule per three graphene hexagons.

The physisorption of nitrogen on graphite can be understood by considering electrostatic effects that influence the adsorption process. A useful analogy is the mirror charge effect, where a charge near a conductor induces an image charge, altering the local electrostatic potential. Although van der Waals forces are the primary drivers of physical adsorption, they exhibit similarities to electrostatic interactions, as both come from fluctuations in charge distribution. To illustrate this, we consider a simplified model: a hydrogen atom near a perfect conductor. This system helps us understand how an adsorbate interacts with a polarizable surface. The system is shown in figure 4.

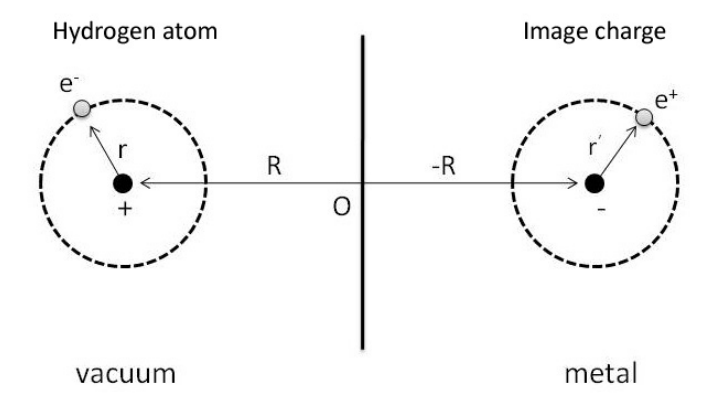


Figure 4. Hydrogen atom and its image near a perfect conductor. Image sourced from [15]. Licensed under CC BY-SA 3.0. No modifications were made.

In this model, the presence of the conductor modifies the electrostatic potential due to the mirror charge effect, wherein the conductor effectively replaces its own response to an external charge with an image charge of opposite sign. This allows us to approximate the interaction energy between the hydrogen atom and the surface. The total electrostatic energy of the system can be expressed as:

$$V = \frac{e^2}{4\pi\epsilon_0} \left(\frac{-1}{|2\mathbf{R}|} + \frac{-1}{|2\mathbf{R} + \mathbf{r} - \mathbf{r}'|} + \frac{1}{|2\mathbf{R} + \mathbf{r}'|} + \frac{1}{|2\mathbf{R} + \mathbf{r}|} \right), \tag{2}$$

where $\mathbf{R} = (0, 0, Z)$ is the position of the hydrogen nucleus relative to the conductor, $\mathbf{r} = (x, y, z)$ is the position of the hydrogen electron relative to its nucleus, and \mathbf{r} is the position of an electron within the conductor. The first two terms in equation (2) correspond to repulsive interactions between like charges (nucleus-nucleus and electron-electron), while the last two terms account for attractive interactions between opposite charges (nucleus-electron).

To obtain an effective interaction potential, we expand equation (2) using a Taylor series in powers of $|\mathbf{r}|/|\mathbf{R}|$, yielding:

$$V = \frac{-e^2}{16\pi\epsilon_0 Z^3} \left(\frac{x^2 + y^2}{2} + z^2 \right) + \frac{-3e^2}{32\pi\epsilon_0 Z^4} \left(\frac{x^2 + y^2}{2} z + z^3 \right) + \mathcal{O}\left(\frac{1}{Z^5} \right). \tag{3}$$

From equation (3), it follows that the interaction potential varies as Z^{-3} , meaning that the attractive interaction between the hydrogen atom and the conductor becomes stronger as the atom approaches the surface. More precisely, this interaction energy corresponds to the difference in zero-point energy between a free atom and an atom near a polarizable substrate [16].

This result has direct implications for the physisorption of nitrogen on graphite. Graphite, though not a perfect conductor, is a highly polarizable material due to its delocalized π -electron system. When a nitrogen molecule approaches the graphite surface, the fluctuating dipole moments of the nitrogen molecule induce image dipoles in the graphite, leading to an attractive interaction similar to the mirror charge effect discussed in the simplified hydrogen model. However, in real physisorption scenarios, this interaction is better described by van der Waals forces, which arise from instantaneous charge fluctuations rather than static electrostatic effects. Nevertheless, the Z^{-3} dependence of the interaction energy provides a useful approximation for understanding the qualitative behavior of adsorption potential wells in physisorption systems.

3.1 Langmuir adsorption model

The most commonly used model for gas-solid adsorption is the Langmuir model that describes mono-layer adsorption on a perfect uniform surface. The model can be based either on kinetic or statistical arguments. This derivation considers statistical arguments. The model describes the adsorption of a single kind of adsorbate onto a series of N equivalent adsorption sites of the solid. We make an assumption that the gas is ideal with the chemical potential μ and that the adsorbed molecule has energy ε_0 compared to one in a free state. The canonical partition function of a system is evaluated as

$$Z_{\mathcal{C}}(N_{\mathbf{a}}) = \frac{N_{\mathbf{m}}!}{N_{\mathbf{a}}! \left(N_{\mathbf{m}} - N_{\mathbf{a}}\right)!} e^{\beta N_{\mathbf{a}} \varepsilon_0},\tag{4}$$

where we have $N_{\rm m}$ adsorption sites on the flat uniform surface and the number $N_{\rm a}$ of those sites are occupied. The $N_{\rm a}$ adsorbed molecules can be arranged among $N_{\rm m}$ available sites following combinatorial principles. The fraction can also be written with the binomial coefficient $\binom{N_{\rm m}}{N_{\rm a}}$. Lastly, $\beta = 1/k_{\rm B}T$, where $k_{\rm B}$ is the Boltzmann constant. From the partition function, we can then write the grand canonical partition function

$$Z_{\rm G} = \sum_{N_{\rm a}=0}^{N} \lambda^{N_{\rm a}} Z_{C} \left(N_{\rm a} \right) = \left(1 + \lambda e^{\beta \varepsilon_{0}} \right)^{N},$$

where λ is referred to as the absolute activity and is related to the chemical potential $\lambda = e^{\beta \mu}$. We can easily calculate the average number of adsorbed molecules

$$\langle N_{\rm a} \rangle = \lambda \frac{\partial \ln Z_{\rm G}}{\partial \lambda} = N_{\rm m} \frac{\lambda e^{\beta \varepsilon_0}}{1 + \lambda e^{\beta \varepsilon_0}}.$$
 (5)

As defined in equation (1) the coverage is

$$\Theta = \frac{\langle N_a \rangle}{N_{\rm m}} = \frac{\lambda e^{\beta \varepsilon_0}}{1 + \lambda e^{\beta \varepsilon_0}}.$$

If we consider that in equilibrium chemical potentials of adsorbed and gas phase are equal, $\mu_a = \mu_g$, therefore $\lambda_a = \lambda_g$ and $\lambda_g = N_g/z_{gas}$, we get

$$\lambda_{\rm gas} e^{\beta \varepsilon_0} = \lambda_a e^{\beta \varepsilon_0} = \frac{N_g}{z_q} z_a,$$

here z_i are partition functions of a certain phase. We considered the gas to be ideal and therefore $pV = Nk_BT$, we get Langmuir adsorption equation [17]:

$$\Theta = \frac{K_{\rm L}P}{1 + K_{\rm L}P}; \quad \text{where } K_{\rm L} = \frac{z_{\rm a}}{z_{\rm gas}} \frac{V}{k_{\rm B}T}, \tag{6}$$

where P represents the partial pressure of the gas phase. This quantity is directly related to the concentration of the gas phase C through the ideal gas law P = CRT, therefore Langmuir equation is often represented as

$$\Theta = \frac{K_{\rm C}C}{1 + K_{\rm C}C}; \quad \text{where } K_{\rm C} = K_{\rm L} \frac{RT}{P}.$$
 (7)

From equation (6) we can see that at low pressures the value $K_{\rm L}P \ll 1$ and Langmuir equation can be simplified to $\Theta \approx K_{\rm L}P$, that being the case we get a linear dependency. On the contrary, at higher pressures $K_{\rm L}P \gg 1$ and $\Theta \approx 1$. In this region, the adsorption capacity approaches a maximum value, known as the mono-layer capacity ($\Theta_{\rm max}$). This represents the saturation point, where all available adsorption sites on the surface are occupied, and a further increase in pressure does not result in additional adsorption.

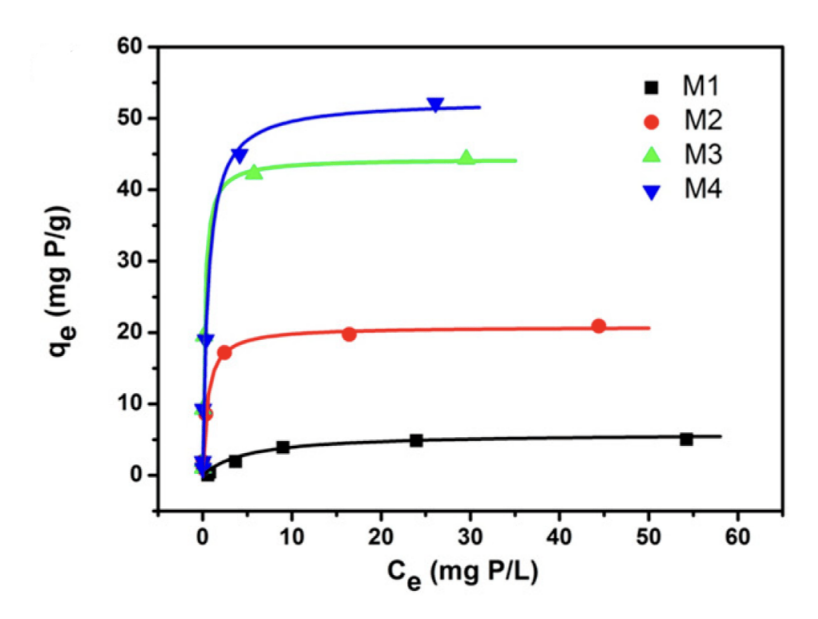


Figure 5. Experimental adsorption data fitted to the Langmuir isotherm model for phosphate adsorption on Fe(III)-coordinated amino-functionalized MCM-41 materials with different amino loadings (0 %, 10 %, 20 %, and 30 %, denoted as M1, M2, M3, and M4, respectively). The x-axis represents the equilibrium concentration of phosphate ions in solution (C_e), while the y-axis shows the amount of adsorbed phosphate per unit mass of adsorbent (q_e). The saturation behavior of the isotherms reflects Langmuir-type monolayer adsorption, with a clear plateau at higher concentrations. Samples with higher amino group content exhibit increased maximum adsorption capacities, consistent with a larger number of available adsorption sites. Adapted from [18], under CC BY 4.0. Modifications were made to crop the image.

The validity of the Langmuir adsorption model has been confirmed experimentally in various systems. Figure 5 shows experimental data of phosphate adsorption on mesoporous MCM-41, a material functionalized with amino groups that serve as adsorption sites for phosphate ions. The four samples, denoted as M1, M2, M3, and M4, contain increasing amino group loadings of 0%, 10%,

20 %, and 30 %, respectively [18]. The x-axis represents the equilibrium concentration of phosphate in solution, $C_{\rm e}$ (mol/L), which corresponds to the concentration C used in equation (7). The y-axis shows the amount of phosphate adsorbed per unit mass of adsorbent, $q_{\rm e}$ (mol/g), which represents the experimentally measured adsorption capacity. This quantity reflects surface coverage and can be seen as the experimental counterpart to the theoretical parameter Θ , scaled by the maximum possible adsorption on the material. Using $q_{\rm e}$ instead of Θ allows the Langmuir model to be fitted to experimental data expressed in terms of adsorbed amount versus equilibrium concentration. The shape of the curves shows a clear saturation trend, with adsorption reaching a plateau at higher concentrations ($C_{\rm e} \gtrsim 10$ mg P/L), consistent with the Langmuir model prediction. Moreover, the maximum adsorption capacity increases with amino group content, following the trend M4 > M3 > M2 > M1. This suggests that a higher density of functional groups leads to a larger number of available adsorption sites.

3.2 Langmuir model modifications

As stated, the basic Langmuir model predicts the surface to be flat and uniform. However, microporous materials are more commonly used in technologies that exploit adsorption. Therefore, we have to modify equation (6) for those instances. Langmuir model for microporous materials follows the same derivation concept as the one for flat uniform surfaces. In this derivation, we will only present the main steps to get to the final equation. The key distinction between derivations is that we now consider a system composed of M cavities or channels. In this case, we are dealing with M-independent open subsystems belonging to the grand canonical potential. Let's assume that each cavity can accommodate a maximum of m molecules. The canonical partition function of a subsystem now changes from (4) to

$$Z_{\mathrm{C}}\left(N_{\mathrm{a}}\right) = \frac{m!}{N_{\mathrm{a}}!\left(m-N_{\mathrm{a}}\right)!} \left(Z_{\mathrm{a}}^{\mathrm{I}}\right)^{N_{\mathrm{a}}} \exp\left[-\beta N_{\mathrm{a}}\left(E_{0}^{\mathrm{a}}+\eta E_{\mathrm{i}}\right)\right],$$

where $Z_{\rm a}^{\rm I}$ is the canonical partition function for the internal degrees of freedom of the adsorbate in the adsorbed phase. The term ε_0 represents the reference energy of an adsorbed molecule in a homogeneous adsorption field inside the cavity, while $\eta \varepsilon_{\rm i} = \frac{cN_{\rm a}}{2m} \varepsilon_{\rm i}$ accounts for the average interaction energy between neighboring adsorbed molecules, assuming a random distribution. The variable c denotes the number of nearest neighbors within a cavity. In order to get the isotherm equation, we have to make one final approximation: $cN_{\rm a}/2m \approx c \langle N_{\rm a} \rangle/2m$. Then by using the first part of the equation (5), we can calculate the isotherm equation:

$$\Theta = \frac{K_{\rm L}'P}{1 + K_{\rm L}'P},\tag{8}$$

where

$$K_L' = \frac{Z_{\rm a}^{\rm I}}{Z_{\rm g}^{\rm I}} \cdot \frac{1}{\Lambda k_{\rm B}T} \exp\left[\beta \left(\varepsilon_0^{\rm g} - \varepsilon_0^{\rm a} + \Omega\Theta\right)\right],\tag{9}$$

where $\Omega=c\,\varepsilon_{\rm i}/2$ and $\Lambda=\left(\frac{2\pi m'k_{\rm B}T}{h^2}\right)^{3/2}$ is the thermal de Broglie wavelength of the gas-phase molecule, with m' denoting its molecular mass and h Planck's constant. The terms $\varepsilon_0^{\rm g}$ and $\varepsilon_0^{\rm a}$ represent the reference energies of the molecule in the gas phase and adsorbed state, respectively. It is also important to note that the exponent in equation (9) reflects the average adsorption potential in the volume occupied by the adsorbed molecules. This potential can be expressed as a function of surface coverage: $\zeta(\Theta)=-\left(\varepsilon_0^{\rm g}-\varepsilon_0^{\rm a}+\Omega\Theta\right)$ [11]. If we compare equations (6) and (8), we observe that they share the same basic mathematical form and both express surface coverage Θ as a function of gas-phase pressure P. However, the key difference lies in the interpretation of the equilibrium

constant. In the classical Langmuir model (6), the constant $K_{\rm L}$ reflects adsorption on an open, flat surface with non-interacting sites. In contrast, the modified model for microporous materials (8) introduces a modified equilibrium constant $K'_{\rm L}$ that incorporates additional interaction terms. These additional terms reflect how molecules interact with each other in confined spaces and how the geometry of narrow pores influences adsorption. Because of this, the effective strength of adsorption can vary noticeably between the two models, even though both show a similar pressure-dependent behavior.

4. Adsorption in electronic nose with capacitive sensors

The electronic nose (E-nose) is a device designed to replicate the olfactory capabilities of the biological nose by detecting and analyzing chemical compounds in the vapor phase. The core of these devices is an array of partially selective chemical sensors, each responding differently to various volatile compounds. The combined output of these sensors forms a unique signal pattern for each odor. By applying pattern recognition algorithms or machine learning techniques, we can interpret these patterns and distinguish between different smells. A key requirement for successful odor discrimination is that the responses of individual sensors are sufficiently uncorrelated, ensuring that the overall response pattern is rich and distinctive. In this section, we focus on a specific class of electronic noses that use capacitive sensors, such as the system developed at the Jožef Stefan Institute (JSI). The working principle of these sensors is closely tied to the adsorption phenomena discussed in Section 3. When vapor-phase molecules come into contact with the sensor array, they adsorb onto the functionalized surface of each capacitive sensor. As adsorption progresses, the dielectric properties of the sensing layer change, which in turn affects the sensor's capacitance. The extent of adsorption, or surface coverage Θ , can be described using adsorption isotherms such as the Langmuir model, introduced in equation (7). In materials with internal porosity, where additional interactions between adsorbed molecules become relevant, a modified Langmuir model (8) provides a more accurate description. Active research on E-nose technology is ongoing at the Jožef Stefan Institute, where a device is equipped with an array of 64 capacitive sensors. Each sensor is functionalized with a different chemical layer to enhance selectivity toward specific analytes. As target molecules adsorb onto these tailored surfaces, they alter the dielectric properties of the sensing layer, resulting in a measurable shift in capacitance. This change in capacitance serves as the measurable output used for compound identification [19].

The experimental setup for this study focuses on detecting volatile organic compounds (VOCs) in exhaled breath to assess their potential as biomarkers for pulmonary cancer. Figure 6a shows the physical implementation of the E-nose, while Figure 6b displays the ceramic gas distribution system, which ensures uniform gas distribution across all sensors in the array.

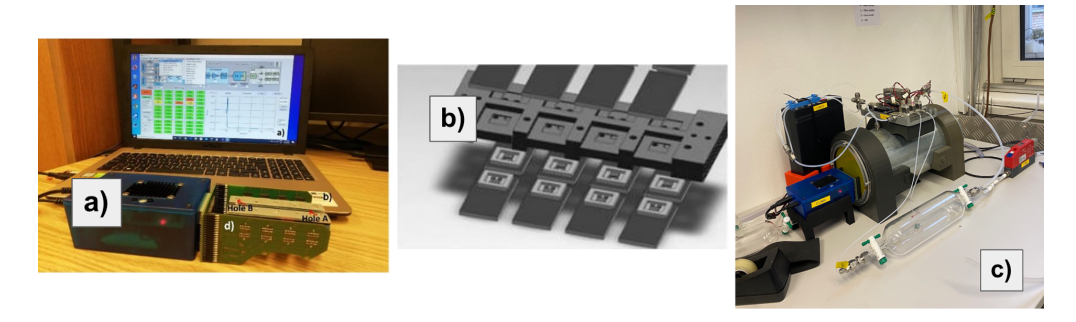


Figure 6. a) Physical implementation of the electronic nose, b) Holder for individual sensors, made of thin ceramic sheets with voids and channels, where the gas is pumped through, c) experimental setup. a) and b) adapted from [19], under CC BY 4.0. Modifications were made to crop the image.

In the current setup, exhaled breath is collected in a glass container (Figure 6c) and compared against a nitrogen reference. The gas mixture is alternately pumped into the system under controlled conditions, inducing cyclic adsorption and desorption on the sensor surfaces. These cycles result in measurable changes in capacitance. The primary extracted feature is the difference in capacitance between the baseline state (under pure nitrogen, corresponding to negligible surface coverage) and the exposed state (under exhaled breath, with higher surface coverage) [20]. Additional features, such as the slope of capacitor charging during exposure, may also provide insight into the kinetics of adsorption. Because each measurement cycle uses a fixed concentration of analyte, higher concentrations generally produce larger capacitance shifts, indicating that more molecules are being adsorbed onto the sensor surface.

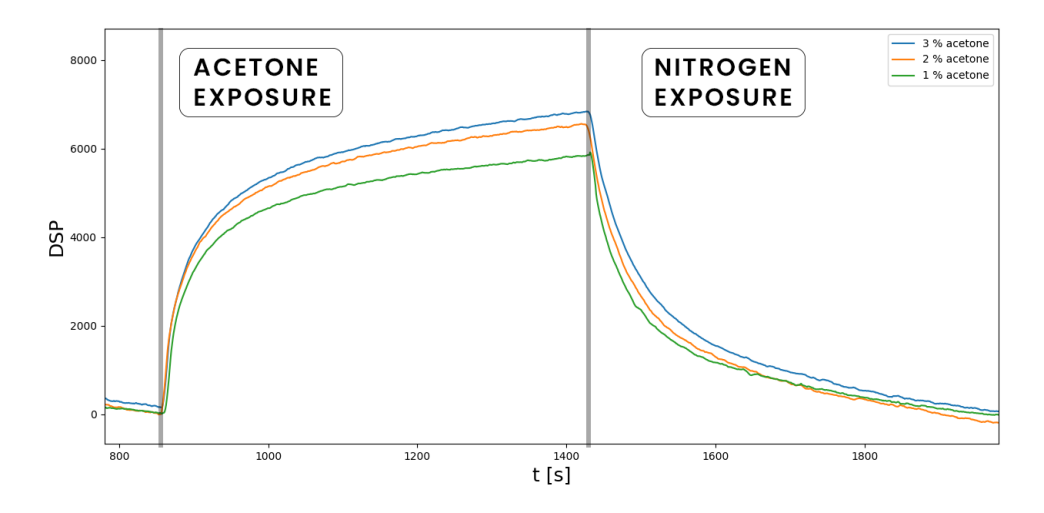


Figure 7. A typical response of a single sensor during the measurement of different acetone concentrations vs the pure nitrogen.

Figure 7 illustrates a typical sensor response over a single measurement cycle, consisting of distinct adsorption and desorption phases. The y-axis is expressed in arbitrary units resulting from digital signal processing (DSP), but these values are directly proportional to the sensor's capacitance. In this experiment, acetone was used as the analyte. As its concentration increases, the signal amplitude grows accordingly, indicating a larger change in capacitance due to increased adsorption. The observed shift corresponds to increased surface coverage by acetone molecules and serves as the key feature for quantifying their concentration. Although only three concentrations are shown, the observed increase in signal amplitude qualitatively reflects the expected trend from adsorption-based sensing where higher analyte concentrations lead to greater surface coverage and thus a larger dielectric response. This behavior aligns with the general principles of adsorption theory. However, a detailed comparison with models such as the Langmuir isotherm would require a systematic measurement across a broader range of concentrations and then plotting the sensor response as a function of analyte concentration. Such an approach would enable a more rigorous validation of model predictions and quantify the extent of nonlinearity in the response curve.

4.1 Potential Improvements to Capacitive Sensor Arrays

The capacitive sensors used in the electronic nose system at the JSI use sensors with interdigitated electrodes, which are covered with a thin layer of SiO₂. Monolayers of selected chemical compounds are then deposited on that surface [19]. This setup enables selective adsorption of specific volatile compounds and reliably produces measurable shifts in capacitance during cyclic exposure to ana-

Adsorption in electronic nose

lytes. However, because the functionalization involves only a monolayer, the surface offers a limited number of adsorption sites per unit area compared to porous materials. According to the Langmuir adsorption model, such surface-limited systems tend to reach saturation quickly, especially at higher analyte concentrations.

To increase sensitivity, a logical next step is to increase the number of available adsorption sites. This can be achieved by functionalizing the sensor surface with porous materials that exhibit extremely high internal surface area, which often exceeds several thousand square meters per gram [21]. This allows for significantly more adsorption sites compared to flat functionalized surfaces. These materials behave according to modified adsorption isotherms, as discussed in Section 3, where adsorption occurs not only on the external surface but also within internal pores, resulting in a higher total adhesion and a smoother progression with increasing concentration. Among them, metalorganic frameworks (MOFs) are particularly promising due to their tunable chemical functionality, high porosity, and ability to selectively adsorb target analytes. Their highly ordered, crystalline structure composed of metal nodes and organic linkers is illustrated in Figure 8. Several studies have demonstrated significant improvements in sensitivity when MOFs are incorporated into capacitive gas sensors [22].

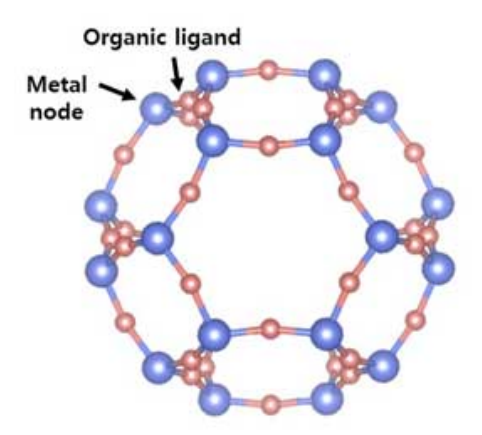


Figure 8. Structural diagram illustrating the porous nature of MOFs, which consist of metal nodes connected by organic linkers, enabling high surface area and selective adsorption properties. Adapted from [23], under CC BY 4.0. Modifications were made to crop the image.

In addition to material selection, the geometry of the sensor electrodes plays a crucial role in how adsorption-induced dielectric changes affect the measured capacitance. The JSI system employs interdigitated electrodes (IDE), where lateral electric fields extend across the surface of the sensing layer. This configuration allows direct exposure of the functionalized surface to analyte vapors and is relatively simple to fabricate. However, due to the open design, some of the electric field lines extend into the substrate and surrounding environment, introducing parasitic capacitance visible in Figure 9. These effects can reduce the sensitivity, especially when using thin or monolayer functionalizations. In the context of porous materials such as MOFs, an alternative electrode geometry has been explored in the literature: the metal-insulator-metal (MIM) structure. Unlike IDEs, the MIM configuration confines the electric field within the sensing layer, providing a more direct and sensitive coupling between adsorption and capacitance change. Comparative studies using ZIF-8 MOF layers in both IDE and MIM setups have shown that MIM structures can significantly increase sensitivity, particularly at low analyte concentrations, due to improved field confinement and minimized parasitic effects [24]. The basic layouts of both IDE and MIM configurations are shown in Figure 9.

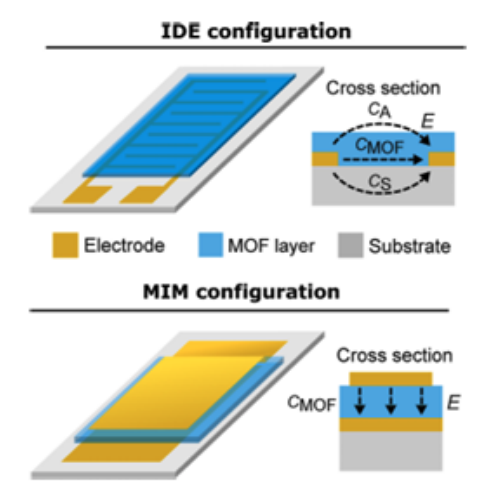


Figure 9. Comparison of interdigitated electrode (IDE) and metal-insulator-metal (MIM) capacitor designs, commonly used in gas sensor applications due to their differing electric field distributions and sensitivity. Adapted with permission from [24]. Copyright © 2023, American Chemical Society.

The integration of porous materials such as MOFs into capacitive sensor designs offers a clear advantage in terms of adsorption capacity and sensitivity, as predicted by adsorption isotherm theory and supported by experimental studies. Despite ongoing challenges, such as ensuring that the films are uniform, stable, and allow gases to reach the active sites, these materials remain a promising path toward more responsive and selective gas sensors. Their use fits well with the adsorption models explored in this article and offers a solid scientific foundation for further improvements in electronic nose technology.

5. Conclusion

In conclusion, we explored the basic properties of adsorption in gas-solid systems. We explored the distinction between physisorption and chemisorption, as well as the significance of mono-layer and multi-layer adsorption. We derived a basic adsorption model and then modified it for microporous materials. We showed that in specific systems, experimental data can be well described by the Langmuir model, allowing the estimation of Langmuir constants through fitting. However, it is important to note that the simple Langmuir model does not accurately describe adsorption on most materials and is only applicable under certain assumptions. The theoretical models discussed in this article also help clarify the role of adsorption in gas sensing, particularly in capacitive sensors integrated in electronic nose systems. In the final part of the article, we focused on capacitive sensor arrays, where adsorption is directly linked to changes in dielectric properties and, consequently, to measurable shifts in capacitance. In the current electronic nose system developed at the Jožef Stefan Institute, the sensors are functionalized with various chemical coatings to improve selectivity for specific analytes. Although MOFs are not yet used in this setup, their high surface area and tunable adsorption behavior make them promising candidates for enhancing sensitivity and overall performance in future sensor designs.

REFERENCES

- [1] C. Cavalcante Jr., Industrial adsorption separation processes: Fundamentals, modeling and applications, Latin American Applied Research 30 (2000).
- [2] J. Kammerer, R. Carle and D. R. Kammerer, Adsorption and Ion Exchange: Basic Principles and Their Application in Food Processing, Journal of Agricultural and Food Chemistry 59 (2011), 22–42.
- [3] V. Blay, L. F. Bobadilla and A. Cabrera García, Zeolites and Metal-Organic Frameworks, Amsterdam University Press, 2018.

Adsorption in electronic nose

- [4] M. M. Sabzehmeidani, S. Mahnaee, M. Ghaedi, H. Heidari and V. A. L. Roy, Carbon based materials: a review of adsorbents for inorganic and organic compounds, Materials Advances 2 (2021), 598–627.
- [5] J. J. Hamon, R. F. Tabor, A. Striolo and B. P. Grady, Atomic Force Microscopy Force Mapping Analysis of an Adsorbed Surfactant above and below the Critical Micelle Concentration, Langmuir 34 (2018), 7223–7239.
- [6] F. Masini, Y. Ning, Z. Li, E. Lægsgaard, F. Besenbacher and T. R. Linderoth, Adsorption of the organic salt TAB(HCl)₄ on Cu(111) studied using STM and XPS, Chemical Communications 49 (2013), 8665–8667.
- [7] H. Ji, W. Zeng and Y. Li, Gas sensing mechanisms of metal oxide semiconductors: a focus review, Nanoscale 11 (2019), 22664–22684.
- [8] H. T. Nagle, R. Gutierrez-Osuna and S. Schiffman, *The how and why of electronic noses*, IEEE Spectrum **35** (1998), 22–31.
- [9] K. Toko, Electronic sensing of tastes, Electroanalysis 10 (1998), 657–669.
- [10] D. García-Toral, R. M. Báez, J. I. Sánchez S, A. Flores-Riveros, G. H. Cocoletzi and J. F. Rivas-Silva, Encapsulation of pollutant gaseous molecules by adsorption on boron nitride nanotubes: A quantum chemistry study, ACS Omega 6 (2021), 14824–14837.
- [11] R. M. A. Roque-Malherbe, Adsorption and diffusion in nanoporous materials, CRC Press, London, 2020.
- [12] J. Rouquerol, F. Rouquerol and K. Sing, Adsorption by powders and porous solids, Academic Press, San Diego, 1998.
- [13] M. Thommes, K. Kaneko, A. V. Neimark, J. P. Olivier, F. Rodriguez-Reinoso, J. Rouquerol and K. Sing, Physisorption of gases, with special reference to the evaluation of surface area and pore size distribution (IUPAC Technical Report), Pure and Applied Chemistry 87 (2015), 1051–1069.
- [14] T. T. Chung and J. G. Dash, N₂ monolayers on graphite: Specific heat and vapor pressure measurements thermodynamics of size effects and steric factors, Surface Science 66 (1977), 559–580.
- [15] Physisorption 1, Wikimedia Commons, The Free Media Repository, accessed 16 Feb 2025, available at https://commons.wikimedia.org/wiki/File:Physisorption_1.jpg.
- [16] A. Zangwill, *Physics at Surfaces*, Cambridge University Press, Cambridge, 2012.
- [17] L. Kolar-Anić, Langmuir and BET adsorption isotherms: Statistical-mechanical derivation, Journal of the Serbian Chemical Society 59 (1994), 433–440.
- [18] X. Chen, Modeling of experimental adsorption isotherm data, Information 6 (2015), 14–22.
- [19] D. Strle, B. Štefane, M. Trifkovič, M. Van Miden, I. Kvasić, E. Zupanič and I. Muševič, Chemical selectivity and sensitivity of a 16-channel electronic nose for trace vapour detection, Sensors 17 (2017), 2845.
- [20] A. Gradišek, M. van Midden, M. Koterle, V. Prezelj, D. Strle, B. Štefane, H. Brodnik, M. Trifkovič, I. Kvasić, E. Zupanič and I. Muševič, Improving the chemical selectivity of an electronic nose to TNT, DNT and RDX using machine learning, Sensors 19 (2019), 5207.
- [21] L. Sarkisov, Accessible surface area of porous materials: understanding theoretical limits, Advanced Materials 24 (2012), 3130–3133.
- [22] Z. Zhai, X. Zhang, X. Hao, B. Niu and C. Li, Metal-organic frameworks materials for capacitive gas sensors, Advanced Materials Technologies 6 (2021), 2100127.
- [23] C. J. Fui, M. S. Sarjadi, S. M. Sarkar and M. L. Rahman, Recent advancement of Ullmann condensation coupling reaction in the formation of aryl-oxygen (C-O) bonding by copper-mediated catalyst, Catalysts 10 (2020), 1103.
- [24] A. Matavž, M. F. K. Verstreken, J. Smets, M. L. Tietze and R. Ameloot, Comparison of thin-film capacitor geometries for the detection of volatile organic compounds using a ZIF-8 affinity layer, ACS Sensors 8 (2023), 3167–3173.